Separation and Purification Technology 288 (2022) 120574

Contents lists available at ScienceDirect

Separation and Purification Technology

journal homepage: www.elsevier.com/locate/seppur

Superhydrophobic ball clay based ceramic hollow fibre membrane via universal spray coating method for membrane distillation

Mohd Haiqal Abd Aziz [a,b], Mohammad Arif Budiman Pauzan [a], Nur Aina Shazana Mohd Hisam [a], Mohd Hafiz Dzarfan Othman [a,*], Mohd Ridhwan Adam [a], Yuji Iwamoto [c], Mohd Hafiz Puteh [d], Mukhlis A. Rahman [a], Juhana Jaafar [a], Ahmad Fauzi Ismail [a], Tonni Agustiono Kurniawan [e], Suriani Abu Bakar [f]

[a] Advanced Membrane Technology Research Centre (AMTEC), School of Chemical and Energy Engineering, Faculty of Engineering, Universiti Teknologi Malaysia, 81310 Skudai, Johor, Malaysia
[b] Department of Chemical Engineering Technology, Faculty of Engineering Technology, Universiti Tun Hussein Onn Malaysia, Pagoh Higher Education Hub, 84600 Panchor, Johor, Malaysia
[c] Department of Life Science and Applied Chemistry, Nagoya Institute of Technology, Gakiso-cho, Showa-ku, Nagoya 466-8555, Japan
[d] School of Civil Engineering, Faculty of Engineering, Universiti Teknologi Malaysia, 81310 Skudai, Johor, Malaysia
[e] College of the Environment and Ecology, Xiamen University (XMU), Xiamen, Fujian Province 361102, PR China
[f] Nanotechnology Research Centre, Faculty of Science and Mathematics, Universiti Pendidikan Sultan Idris, 35900 Tanjung Malim, Malaysia

ARTICLE INFO

Keywords:
Superhydrophobic surfaces
Hierarchical composite
Ceramic membrane
Membrane distillation
Desalination

ABSTRACT

In this work, the feasibility study of a superhydrophobic ball clay based ceramic hollow fibre membrane (HFM) through pre-fluorinating of poly(vinylidene fluoride)–co-hexafluoropropylene (PVDF-HFP) and ZnO nanoparticles composite with 1H, 1H, 2H, 2H-perfluorooctyltriethoxysilane (C8) followed by post-roughening on fluorinated ball clay based ceramic hollow fibre membrane (PH/C8/ZnO-C8/HFM) via universal spray coating. The coating was applied onto ball clay based ceramic hollow fibre membrane's surface in order to achieve superhydrophobicity, which had not previously been reported. C8 was grafted on the ceramic hollow fibre membrane's surface using the conventional immersion method and the prepared membrane (C8/HFM) was served as a control. The hierarchical structure of PH/C8/ZnO-C8/HFM is composed of a cooperative layer of fluorinated PVDF-HFP/ZnO nanocomposite in mechanical interlocking mode. PH/C8/ZnO-C8/HFM has better superhydrophobic properties, with a water contact angle of 154.4° and a hysteresis contact angle of 3.2°, than C8/HFM, which has a water contact angle of 151.7° and a hysteresis contact angle of 9.2°. The PH/C8/ZnO-C8/HFM outperforms the C8/HFM in the wetting resistance because the liquid entry pressure of water LEPw (PH/C8/ZnO-C8/HFM = 1.33 ± 0.4 bar, C8/HFM = 0.37 ± 0.1 bar) and salt rejection in MD for the PH/C8/ZnO-C8/HFM is better than C8/HFM.

1. Introduction

In recent decades, the world's water demand has dramatically increased with the increasing global population. Climate change, poor water resource management, global population growth, and industrial expansion have not only exacerbated water scarcity, but also limited clean water supply [1,2], Access to clean water resources is essential for our survival and for industrial activities. To meet the global demand for fresh water, new water technologies must be put in place to preserve natural water resources and reuse treated wastewater. One of the appealing solutions to water shortage is the use of desalination technologies to desalt seawater in order to ensure a sustainable water supply in many parts of the world [3]. Although various technologies are available to achieve an efficient treatment of wastewaters, membrane distillation (MD) seems to be a promising alternative for the production of sustainable freshwater over the pressure-driven desalination technology. This is due to the fact that MD technology has distinct advantages such as being capable of utilising low-grade thermal energy, operate at low pressure and having a low capital cost due to its high modularity [4–7].

* Corresponding author.
E-mail address: hafiz@petroleum.utm.my (M.H.D. Othman).

https://doi.org/10.1016/j.seppur.2022.120574
Received 17 November 2021; Received in revised form 20 January 2022; Accepted 23 January 2022
Available online 4 February 2022

Table 1
Ball clay composition.

Ball Clay	Al_2O_3	SiO_2	K_2O	CaO	TiO_2	Fe_2O_3	Others
Composition (wt%)	41.6	53.8	1.9	0.12	1	1.1	0.48

However, large-scale industrial implementation of the technology cannot be fully achieved yet as there are still some technical challenges. One of the bottlenecks is due to membrane wetting, of which the penetration of the feed solutions into membrane pores will lead to either permeate flux reduction or permeate quality deterioration. The former results from vapour channel-blocking, while the latter is attributed to full wetting [8]. Another primary cause of wetting is fouling. Material deposition on a membrane's surface or inside a membrane's pores can impair the membrane's hydrophobicity, clog the pores, and damage the membrane, leading to a decline in permeate flux and water quality [8]. Surfactants and/or organic compounds, which reduce the surface tension of the feed solution, could induce wetting by causing the feed-membrane surface to become hydrophilic from surfactant adsorption or through its affinity with the hydrophobic membrane [9]. Many efforts have been made to overcome these bottlenecks including pre-treating the feed, increasing the feed's flow rate, incorporating membrane cleaning, and preparing novel membranes [10]. Among those strategies, the development of a robust membrane with antifouling and antiwetting properties is imperative for a stable MD performance without increasing the treatment cost.

By developing an extremely water repellent surface, fouling and wetting in membrane can be minimized. Superhydrophobic surfaces with water contact angle above 150° and contact angle hysteresis below 10° can repel water effortlessly with self-cleaning properties [11–13]. Synergizing between the construction of surface roughness and the subsequent fluorosilane modification has been the typical approach of fabricating superhydrophobic membranes for membrane distillation. However, the fabrication method varies according to the substrate, which is either inorganic membranes or polymeric membranes. So far, the most recent advances in superhydrophobic modification has been focused on deformable substrates like polymeric membranes and glass fibre membranes. Ceramic membranes, on the other hand, are scarce, despite being ideal substrates (outstanding thermal, mechanical, and chemical stabilities) for robust MD applications [14–17].

To date, most of the ceramic membranes directly render the hydrophilic ceramic membranes hydrophobic through fluorination process [18] and the membranes do not seem to reach extreme water repellence as most of the water contact angle result was less than 150° [19]. Some studies have demonstrated the applicability of developing hierarchical structure for superhydrophobic ceramic membranes but the methods involve high-temperature synthesis [20–22] . For instance, Li et. al. [20] created a ceramic membrane with α-Si_3N_4 nanowires by tape casting silicon slurry, followed by calcination at 1300 °C in flowing NH_3 gas and further modification with dimethyldichlorosilane and dichloromethylsilane, heated to two stages of different temperature (320 and 600 °C) in flowing NH_3 gas. Meanwhile, Chen et. al. [23] deposit ZnO nanorods and nanoparticles on alumina hollow fibre membranes via chemical bath deposition methods followed by surface grafting with fluoroalkylsilane. Other studies have used hydrothermal method to grow ZnO nanorods [21] and TiO_2 microflowers [22], with elevated temperatures during the hydrothermal synthesis with post fluoroalkylsilane grafting.

Surface coating with composite composed of polymer, low surface energy material, and nanoparticles seems to be simpler for the development of superhydrophobic membrane. Composite of polymer and hydrophobic modified nanoparticles (NPs)-embedded polymeric membranes have been noted for their ability to confer anti-wetting and anti-fouling properties [24,25]. Among many nanoparticles, ZnO nanoparticles is a promising roughening agent for a composite due to their desirable shape, great quality, high amount of surface area per unit volume, resistance to heat, stable in harsh operational conditions and stronger bactericidal property when compared to SiO_2 and TiO_2 [26]. Commonly, the composite coating of nanoparticles, polymer and low surface energy material can be applied on membrane surface through either electrospraying [24,26], spraying [27] or dip-coating method [28]. Among them, universal spray coating method appears to be a simpler and more efficient way to develop superhydrophobic membrane, however, its use in fabricating superhydrophobic ceramic membranes has not been reported in the literature.

It is widely known that ceramic membranes can withstand more difficult conditions than their polymeric counterparts [29]. However, ceramic membranes are costly [30] but can be substitute with natural occurring clay. Ball clay, for example, is a promising material for constructing ceramic membranes due to its low cost, and its thermal decomposition produces mullite [31]. Ball clay is largely made up of SiO_2 and Al_2O_3, with a small amount of metal oxide impurities [32]. At high temperature, silicates react with the alumina component to form mullite [31]. Mullite's exceptional thermal and mechanical properties enable it to be used as an alternative material to more expensive ceramics (e.g., Al_2O_3) in the fabrication of ceramic membranes [31].

To bridge the existing research gaps in the body of literature, in this work, the applicability of using a simple spray-coating technique on ball clay based ceramic hollow fibre membrane was investigated to achieve superhydrophobicity for membrane distillation application, which had not previously been studied. The coating composition was based on previous work by Deka et al [26], but the coating was applied using universal spray coating on ceramic membrane. The distribution of PVDF-HFP, fluoroalkylsilane and ZnO nanoparticles composite was evaluated at different spray time and spray cycles. The surface morphology of the modified and unmodified surfaces with the composite were characterized using scanning electron microscopy (SEM). Fourier-transform infrared spectroscopy (FTIR), energy dispersive X-ray (EDX) analysis and X-ray diffraction (XRD) were used to analyse the composition of the samples. The wetting properties of different polarity fluids (e.g: oil, and water) were investigated using a contact angle goniometer. Finally, flux and rejection studies using saline as the feed sample were carried out via a direct contact membrane distillation (DCMD) set-up.

2. Methodology

2.1. Materials

Ball clay with an average of 2 μm particle sizes was obtained from Zibo All Way Import & Export Co., Ltd in China and the elemental composition is shown in Table 1. The solvent, N-methyl-2-pyrrolidone (NMP) was supplied by Merck. The polymer binder, polyethersulfone (PESf) and the dispersant, polyethyleneglycol-30 dipolyhydroxystearate (Arlacel) were purchased from Sigma Aldrich and Croda, respectively. Zinc oxide (ZnO) was purchased from Sigma Aldrich. The solvent, N, N-dimethylformamide (DMF) was supplied by Merck. PVDF-HFP (PH) was obtained by Merck. The silane agent, C8 was purchased from Sigma Aldrich. Ethanol was produced by Merck. Sodium chloride (NaCl) was purchased from R&M Chemicals and sodium dodecyl sulphate (SDS) was purchased from Sigma Aldrich. Palm oil and silicon oil were obtained from Saji Malaysia and Chiptronics (M) Sdn. Bhd., respectively.

2.2. Membrane fabrication

Ceramic hollow fibre membrane fabrication in this work employed the spinning/phase inversion and sintering techniques (see Fig. 1**(a)**) [22]. The ceramic suspension was made by dissolving 1 wt% Arlacel in NMP (34 wt%). After that, 60 wt% ball clay was added to the solvent before the mixture was milled for 2 h in a planetary ball mill (Mvlab XQM-4A, Malaysia). Following the addition of 5 wt% PESf, the mixtures were milled for another 24 h to achieve homogeneity. The ceramic

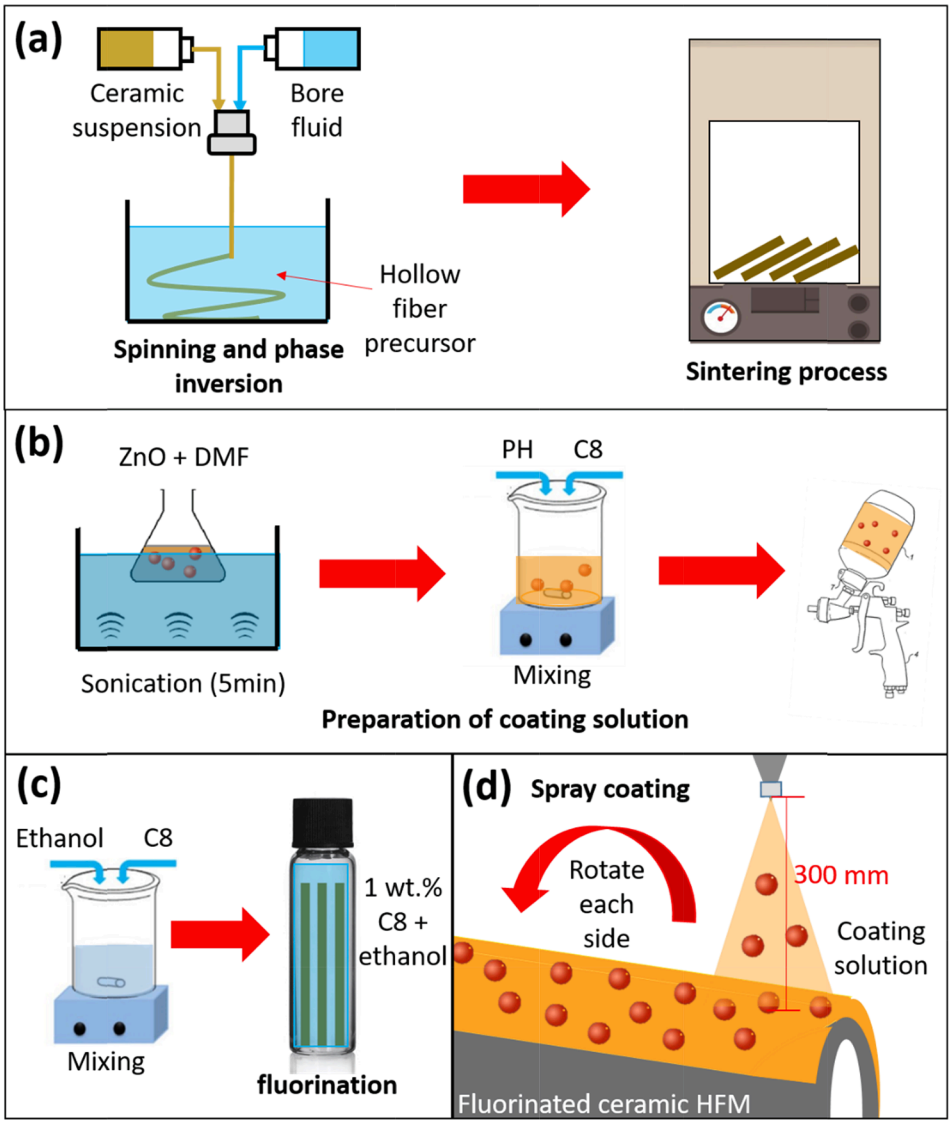

Fig. 1. **(a)** Fabrication of hollow fibre membrane, **(b)** preparation of superhydrophobic coating, **(c)** fluorination process and **(d)** spray coating on a surface of fluorinated hollow fibre membrane.

Table 2
Composition of coating solution for PH/C8/ZnO-C8/HFM.

Materials	Composition
DMF	100 mL
PVDF-HFP	3% (w/w) of DMF
ZnO	30% (w/w) of PVDF-HFP
C8	1% (v/v) of DMF
Ethanol/Water	1:2 (v/v) (50:100 mL) of 150 mL

suspension was then transferred to a stainless-steel syringe and extruded through a tube-in-orifice spinneret at a constant speed of 20 mL/min at 25 °C with bore fluid at a constant speed of 10 mL/min at 25 °C by using syringe pump (Perkin Elmer, U.S.A.) After that, the hollow fibre precursor was immersed in tap water overnight to ensure that the solvent/non-solvent exchange was complete. After that, the hollow fibre precursor was dried at room temperature. The hollow fibre precursor was then dried at ambient temperature. The precursor was sintered in a muffle furnace (Nabertherm, Germany). The sintering profile was as follows: To completely remove the organic polymer binder, the precursor was sintered from room temperature to 600 °C at a rate of 2 °C/min for 2 h. The sintering process was then continued by raising the temperature to 1350 °C at a rate of 5 °C/min and holding it there for 10 h to consolidate the ceramic hollow fibre membranes. It was then cooled down to room temperature.

2.3. Membrane coating

The coating composition is in accordance to the previous study [26]. ZnO was sonicated using ultrasonic sonicator probe (FS-250 N Ultrasonic processor) in DMF for 5 min (20 kHz, 80 W) for complete dispersion. PVDF-HFP (PH) was then vigorously mixed into a homogeneous ZnO-DMF solution for 12 h at 65 °C, followed by the addition of a small amount of C8 and continued mixing for another 30 min. The formulation of the coating solution is as follows (Table 2).

Before surface coating with the composite of PVDF-HFP, ZnO and C8, the sintered hollow fibre membrane was first hydroxylated by immersing it in a solution of ethanol:water, 1:2 (vol:vol) for 24 h. It was then dried at room temperature before being immersed in a C8/Ethanol (1% vol/vol) solution for another 24 h to fluorinate the surface. The C8 coated hollow fibre membrane was then washed with ethanol, followed by drying in the oven (Memmert) at 60 °C overnight. PH/C8/ZnO composite was introduced on fluorinated ball clay based ceramic hollow fibre membrane through spray coating via spray gun (Viderttels) (see

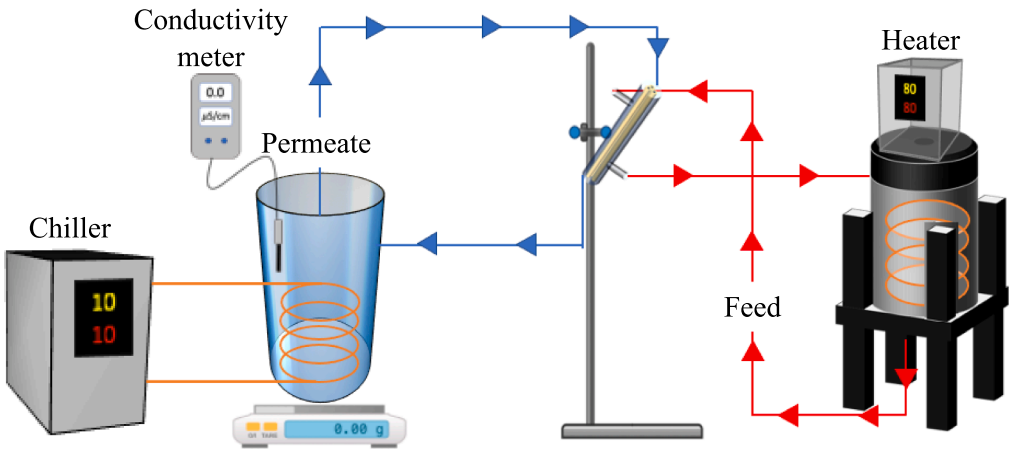

Fig. 2. Schematic diagram of direct contact membrane distillation (DCMD) system set-up.

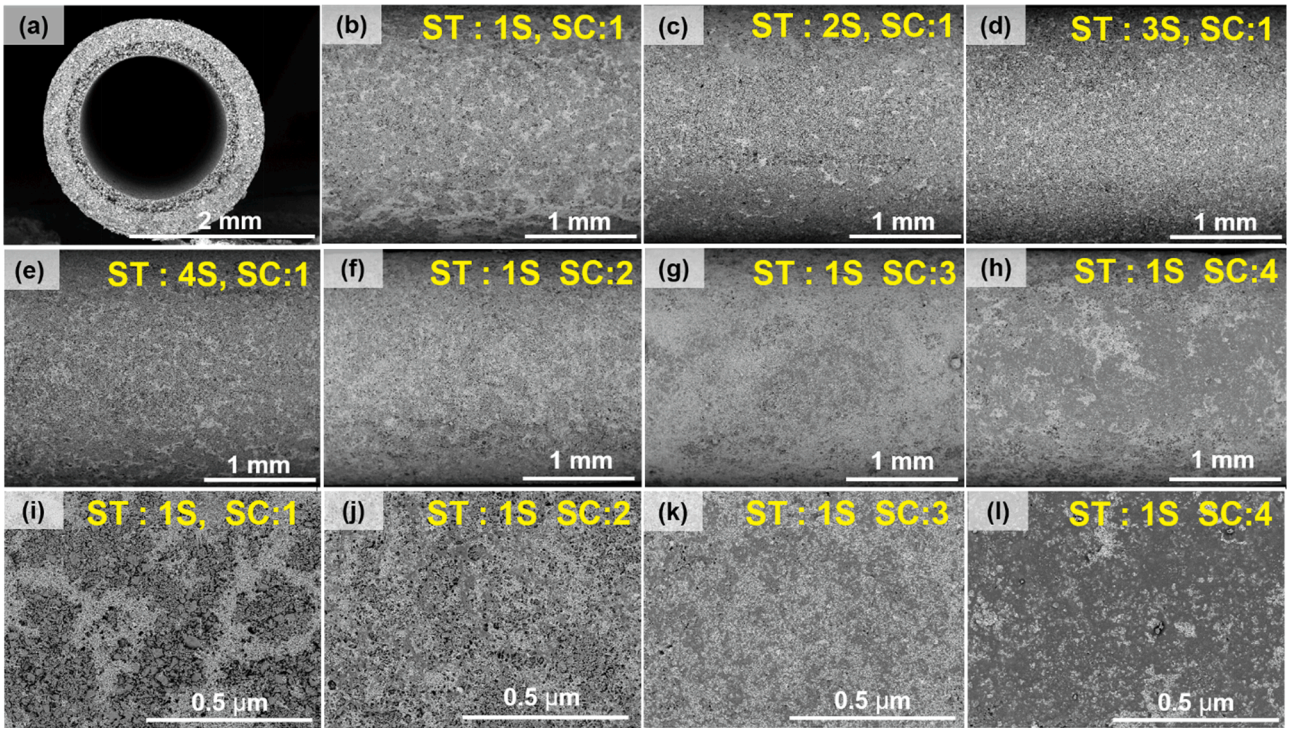

Fig. 3. SEM image showing (a) hollow fibre configuration consisting of sponge layer originating from outer surface and micro-void layer originating from inner surface, (b-e) spray coating between 1 s and 4 s at 1 cycle and (f-h) 1 s-spray coating between 2 and 4 cycles and (i-l) 1 s-spray coating between 1 and 4 cycles at higher magnification. ST is denoted as spray time meanwhile SC is denoted as spray cycle.

Fig. 1**(b-d)**) and denoted as PH/C8/ZnO-C8/HFM. The hollow fibre membrane was subjected to various coating holding times (1 s, 2 s, 3 s, and 4 s) in order to determine the best holding time for ensuring uniformity of the coating solution onto the membrane's surface. The uniformity of the coating solution was investigated further by varying the coating cycle of the chosen holding time from 1 to 4 min. At each spray cycle interval, the coated hollow fibre membrane is dried in the oven for 2 h at 60 °C. The spray coater's nozzle will be held 300 mm away from the hollow fibre membrane, and the membrane will be rolled four times to ensure that each side is coated. C8 modified ball clay based ceramic hollow fibre membrane was served as a control.

2.4. Characterization

A field emission scanning electron microscope, FESEM (SU8020, Hitachi) and a scanning electron microscope, SEM equipped with energy dispersive X-ray, EDX (TM3000, Hitachi) were used to study the surface morphology of the fabricated membranes, with platinum as the surface coating. The surface chemistry of the samples was investigated using Attenuated Total Reflectance-Fourier transform infrared spectroscopy, ATR-FTIR (Nicolet iS10, Thermo Scientific). Thin-film X-ray powder diffraction, XRD (Rigaku Smart Lab) was used to assess the crystallinity in samples over a range of 2 θ values from 5 to 100. The surface topologies were investigated using an atomic force microscopy, AFM (JPK Nanowizard) in the non-contact mode to scan an area of 10 µm × 10 µm. The surface wettability of samples was evaluated at room temperature (25 °C) by measuring contact angles of water and low surface tension liquids using a goniometer (Data Physics Instruments, OCA series). A high-speed camera was used to record the contact angle of one µL of liquid dropped onto the samples as soon as it was dropped. By increasing

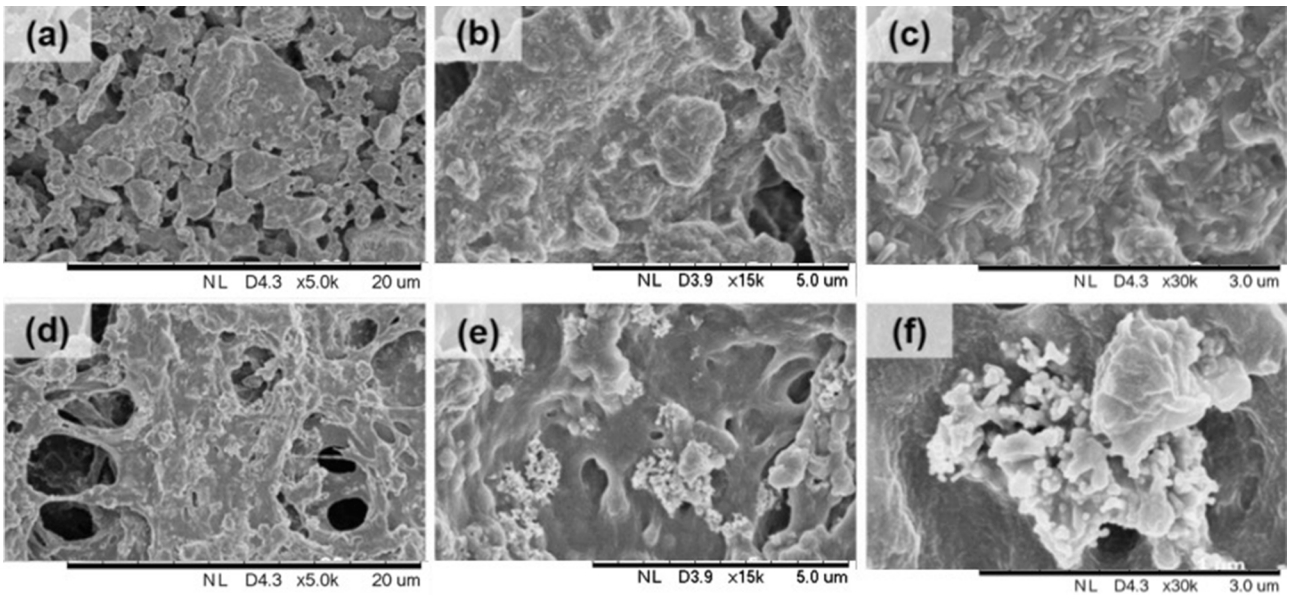

Fig. 4. Surface morphology of (a-c) C8/HFM and (d-f) PH/C8/ZnO-C8/HFM at 3 different magnifications i.e. 5, 15 and 30 k.

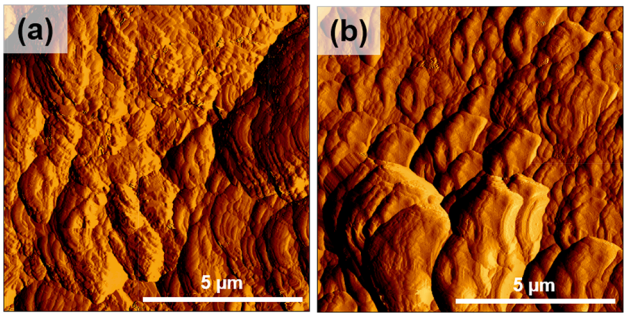

Fig. 5. AFM analysis on C8/HFM and (b) PH/C8/ZnO-C8/HFM.

and decreasing the drop volume by one μL, the advancing and receding contact angles were determined. To test the wettability of membrane samples, polar liquids such as water/ethanol mixtures (0, 10, and 30% ethanol) and ethylene glycol, as well as non-polar liquids such as palm oil and silicon oil, were used. Mercury intrusion porosimetry, MIP (Micromeritics AutoPore IV) was used to characterize the membranes in term of pore structure (pore size and total porosity).

Liquid entry pressure (LEPw) was used to measure the wettability properties of the modified membranes. Referred to previous study by Hubadillah et al [33], about 4 cm membrane length were potted on an adaptor and the end of the membranes were sealed with epoxy, which was later plugged-in to a tank containing distilled water equipped with diaphragm pump and pressure gauge. Followed by circulating distilled water through the lumen side of the membranes and then the pressure in the system was gradually increased by adjusting the valve connected to the pressure gauge. The experiment continued until the first droplet of water was observed on the entire shell side (surface) of the membrane. The experiment was replicated for at least five independent measurements at different spots of each sample of fibre. The first droplet started to appear on the membrane's surface at respective pressure was referred as the LEPw for a given membrane sample. The value of LEPw was determined and recorded in bar unit at increasing 0.1 bar interval.

2.5. Direct contact membrane distillation

The surface modified hollow fibre membranes were tested for 300 min in an in-house direct contact membrane distillation (DCMD) system with a feed stream of 10 g/L NaCl solution [34]. The schematic diagram of the system is shown in Fig. 2. The temperatures of the feed and permeate were set to 80 °C by using heater and 10 °C by using chiller, respectively, which connected to the respective tank. In order to obtain flux and rejection results, the mass and conductivity of permeate were continuously recorded from weighing balance (AND, GF-8000) and conductivity meter (Thermo Scientific, Eutech), respectively. An in-house membrane module used to install the hollow fibre membranes was created from a 20 cm long acrylic tube with two holes in between. After inserting three hollow fibre membranes into the module, the silicone mould was used to seal both ends of the tube without obstructing the membranes' lumen, leaving an effective length of hollow fibre around 15 cm. The tee connectors were inserted into the tube which were placed at both holes and were tightened with nuts. The feed flow (hot) and permeate flow (cold) were flowing through the shell and lumen sides, respectively in a cross-flow mode.

The permeate vapor flux (J, kg/m^2.h) was calculated by the following equation [35]:

$$J = \frac{\Delta W}{A \Delta t} \tag{1}$$

ΔW is the quantity of distillate (kg), A is the effective area of hollow fibre membrane (m^2) and Δt is the sampling time (h). The rejection (R, %) was calculated based on the following equation:

$$R(\%) = \frac{C_f - C_p}{C_f} \tag{2}$$

Where C_f and C_p are the conductance of feed and conductance of permeate, respectively.

3. Results and discussion

3.1. Morphology

Fig. 3**(a)** shows the ceramic membrane prepared from ball clay in hollow fibre configuration consisting of sponge layer originating from outer surface and micro-void layer originating from inner surface. The membrane is then subjected to surface modification, and the distribution of the PH/C8/ZnO layer on its surface at four different spray times (1 s, 2 s, 3 s, and 4 s) is depicted in Fig. 3**(b-e).** At the microscopic level, the coating layer are joined by sporadic interconnecting ridges that cover

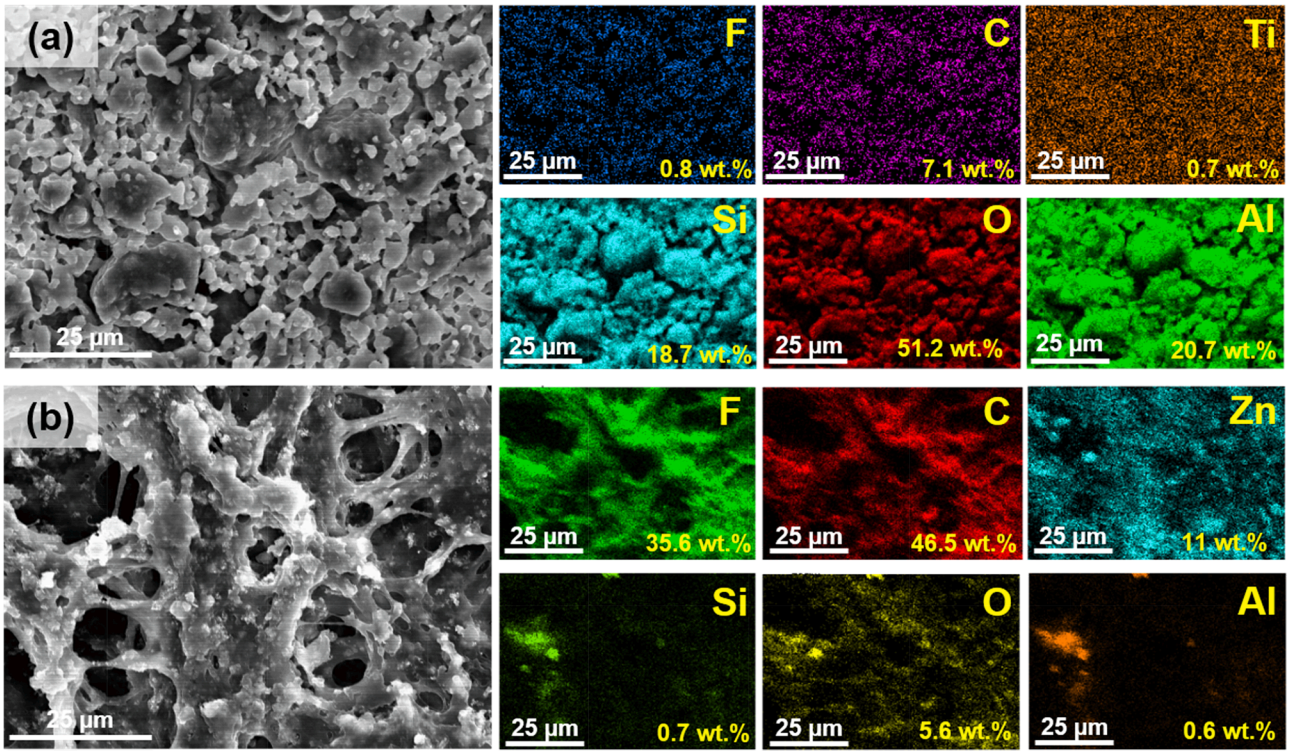

Fig. 6. EDX mapping of (a) C8/HFM (b) PH/C8/ZnO-C8/HFM.

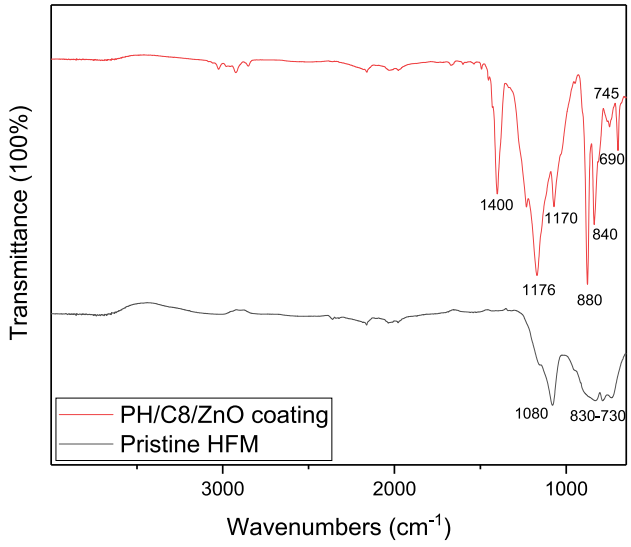

Fig. 7. ATR-FTIR spectra of pristine HFM and PH/C8/ZnO coating layer.

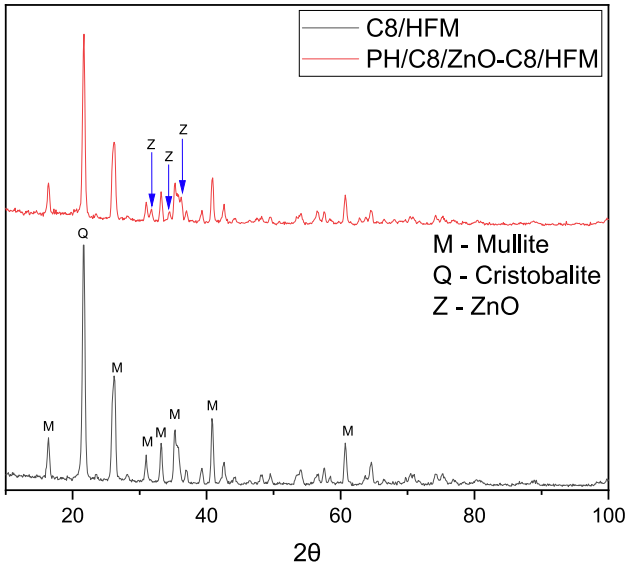

Fig. 8. XRD peak of C8/HFM and PH/C8/ZnO-C8/HFM.

the entire surface of the membrane. Surprisingly, the distribution of the PH/C8/ZnO layer decreased with each spray time. It was postulated that the high strength and flow of the PH/C8/ZnO coating from the 550 W powered spray gun over a long period of time can cause the mixture to spread in a non-uniform pattern distribution on the surface. The shortest spray time, 1 s, produced the best results among the four different spray times because the coating layer covered more of the membrane's surface. Then, multiple spray cycles were conducted to improve the distribution of the PH/C8/ZnO layer, and the resulting morphologies are shown in Fig. 3 **(f-h).** As shown in Fig. 3 **(i-j)**, the PH/C8/ZnO layer distribution does not completely cover the surface of the hollow fibre membrane during the first and second cycles, as the pores and grains can still be seen. The coating layer begins to cover the entire surface evenly after three spray cycles (see Fig. 3**(k-l)**); however, at four cycles, the coating layer becomes too dense. Thereby, in this study, the ideal result was chosen after spraying the substrate three times with a PH/C8/ZnO and the sample is subjected to further studies.

The SEM images (Fig. 4**(a-c)**) reveals that the surface of the ball clay based ceramic hollow fibre membrane substrate is irregular and has a multi-granulous structure. In another sample, a homogeneous mixture of PVDF-HFP, C8 and ZnO nanoparticles was sprayed onto the substrate of ball clay based ceramic hollow fibre membrane to create additional secondary structure. As shown in Fig. 4**(f)**, the ZnO nanoparticles were successfully anchored on the PVDF-HFP network using the spray coating approach. PH/C8/ZnO-C8/HFM showed hierarchical textures (see

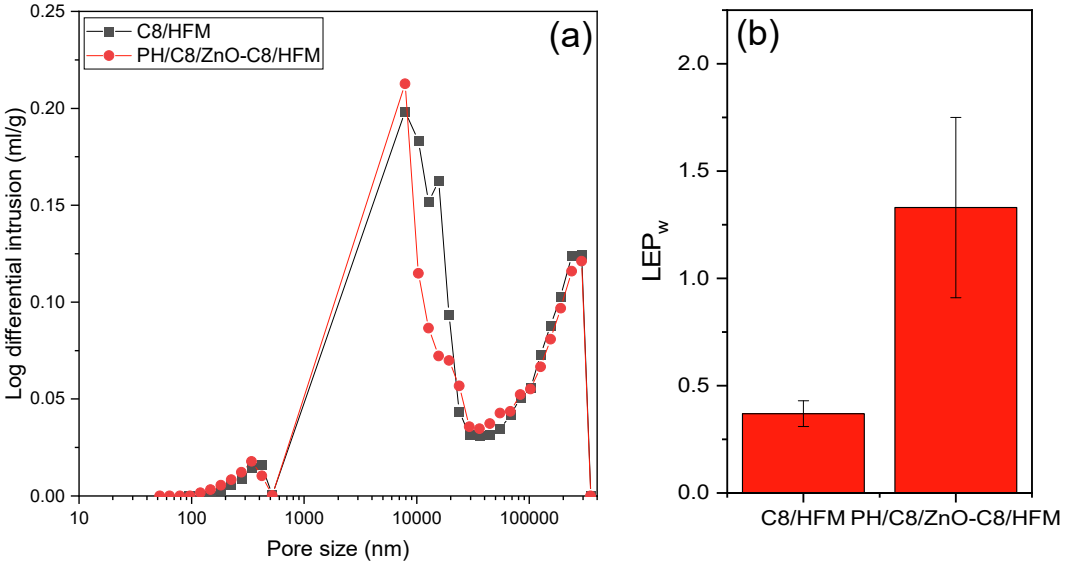

Fig. 9. **(a)** MIP analysis and **(b)** LEP_w results of C8/HFM and PH/C8/ZnO-C8/HFM.

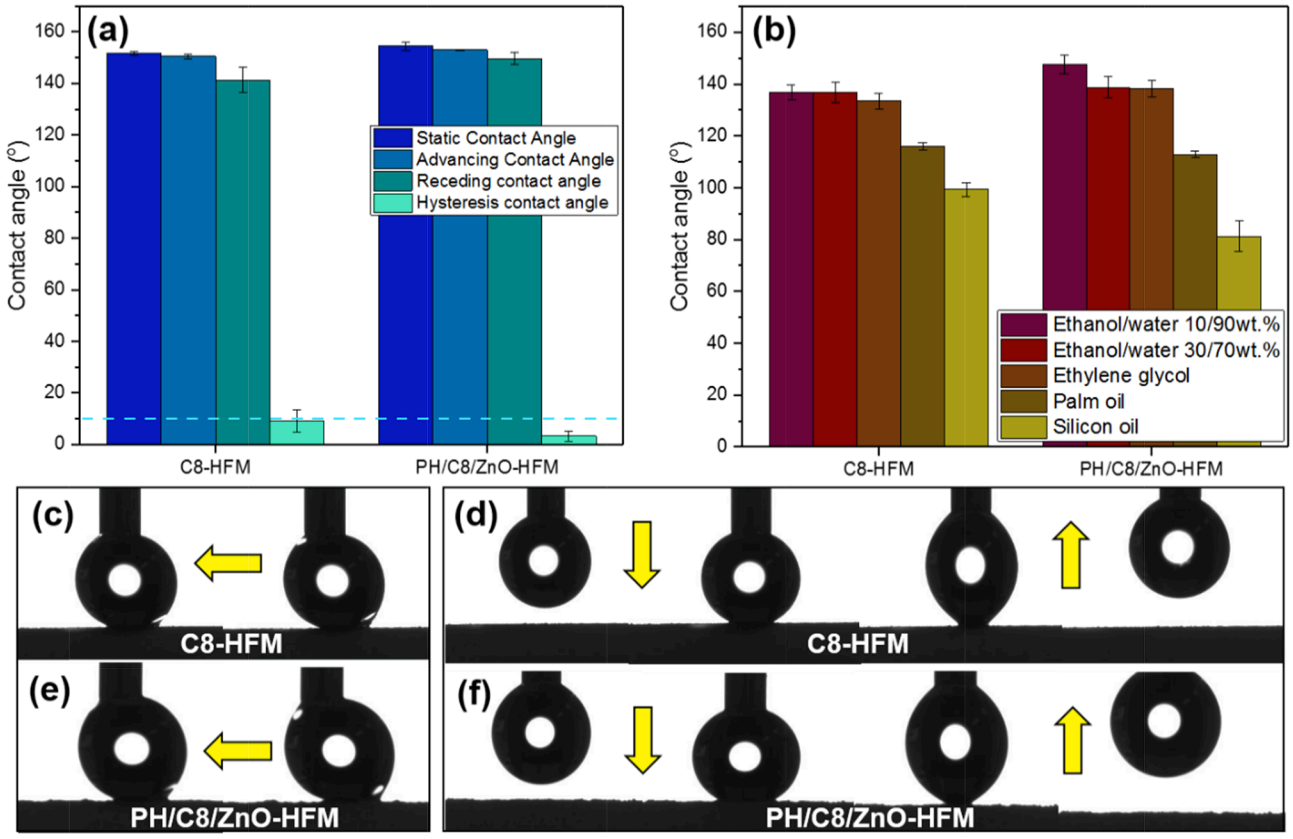

Fig. 10. **(a)** apparent, advancing, receding and hysteresis water contact angle, **(b)** apparent contact angles with low surface tension liquids and **(c-f)** water drop test on C8/HFM and PH/C8/ZnO-C8/HFM.

Fig. 4**)** that is made up of cooperative layer of adhesive PVDF-HFP and ZnO nanoparticles in mechanical interlocking mode. However, the ZnO nanoparticles were not continuously adhered but instead clustered randomly on the PVDF-HFP. We then use AFM to assess their surface roughness, and the results are shown in Fig. 5**.** Both samples have ridge-and-valley structure on their surfaces, but the PH/C8/ZnO-C8/HFM sample has a more clustered ridge-and-valley structure, which is likely due to the aggregates of composite ZnO nanoparticles. The PH/C8/ZnO-C8/HFM surface has a Ra of 4.239 μm, which is greater than that of the C8/HFM surface, which is 2.557 μm.

3.2. *Surface chemistry*

The EDX element mapping reveals that the majority of the substrate's elements are alumina, silica, and other oxides, but their spectrum intensity decreases after surface coating with a PH/C8/ZnO layer as shown

Table 3
Comparison of MD desalination using ceramic membranes.

Year	Material	Membrane Configuration	Surface Modification/ Water contact angle	MD types	Feed/permeate temperature (°C)	Flux (L/ m^2h)	Salt Rejection (%)	Ref.
2016	Alumina-kaolinite clay	Hollow fibre	C8/145°	AGMD	ΔT:60	0.2–4.1	99.1 – 100	[52]
2017	β-Sialon	Planar	SiNCO/~140°	SGMD	60–90/-	2.2–14.1	>99	[53]
2017	Silica	Nano-fibrous	C8-SiO_2/154°	DCMD	60/20	21.9	100	[54]
2018	Rice husk ash	Hollow fibre	C8/157-161°	DCMD	60/10	38.2–52.4	>99.9	[55]
2018	Alumina	Hollow fibre	C8-ZnO/>150°	DCMD	70/15	~14.0	>99.9	[23]
2018	Silica	Planar	DMC/DCM-Si_2N_2O/160°	SGMD	60–90/-	~1.9–11.1	>99.9	[51]
2019	Alumina/silica/ calcium carbonate	Tubular	PPFDA/154-161°	AGMD	~40–80/20	~0.3–3.8	>99.9	[56]
2019	Ytrium silicate	Planar	SiNCO/132°	SGMD	90/-	10.7	>99.9	[57]
2019	SiOC	Planar	SiOC/163°	SGMD	55–85/	~4.0–12.0	>94.6	[58]
2020	Alumina	Tubular	TCS/145°	VMD	70/-	21.5–31.2	>99.9	[59]
2021	Natural Tunisian sand	Tubular	C8/117°	AGMD	85/5	150	~99	[60]
2022	Ball clay	Hollow fibre	C8/>150° PH/C8/ZnO/>150°	DCMD	80/10	Avg, 6.2 Avg, 3.4	>99.8	This work

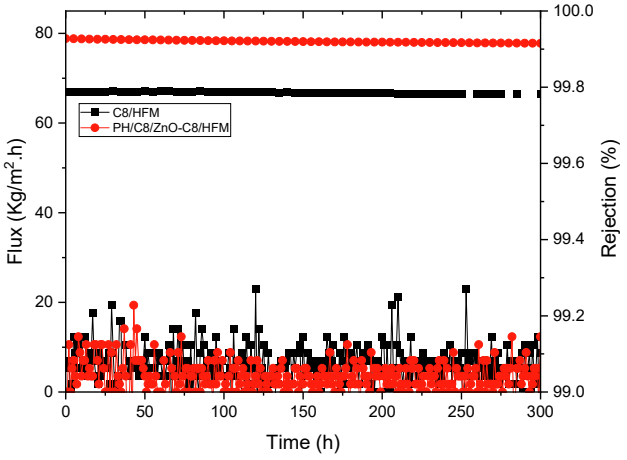

Fig. 11. Vapour flux of C8/HFM and PH/C8/ZnO-C8/HFM via DCMD test with feed of 10 g/L NaCl and rejection of C8/HFM and PH/C8/ZnO-C8/HFM via DCMD test with feed of 10 g/L NaCl.

in Fig. 6. The elements fluorine, carbon, zinc, and oxygen are evenly distributed on the surfaces of the substrate hollow fibre membrane, indicating that the surface of the membrane has been successfully modified with adhesive PVDF-HFP as shown in Fig. 6 **(a-c)** and composite C8-ZnO nanoparticles after spray coating as shown in Fig. 6 **(d-f)**.

Fig. 7 depicts an ATR-FTIR analysis of the chemical properties of the PH/C8/ZnO layer and the hollow fibre substrate. The peak at 1400 cm^{-1} are characteristic to the CH_2 wagging of PVDF-HFP/PVP [36,37] and the band at 745 cm^{-1} are attributed to the CH_2 rocking vibration [37]. The bands at 1176 cm^{-1} may correspond to the stretching of CF_2 [38,39], meanwhile the peak at 1170 cm^{-1} can be assigned to the C-C bond [39]. All the aforementioned peak locations correspond to the adhesive PVDF-HFP and hydrophobic C8. On the other hand, the band at 690 can be corresponded to the Zn-O-Zn antisymmetric and symmetric vibrations of ZnO [40,41] coming from the ZnO nanoparticles anchored on the adhesive layer. The two peaks at 880 and 840 cm^{-1} corresponded to the amorphous and β-phase of the PVDF-HFP, respectively [42]. All the peaks associated with the hollow fibre membranes are also detected on the spectrum namely Si-O-Si (1080 cm^{-1}) and Al-O-Si (750 cm^{-1}) [31,43].

The surface chemical composition of C8/HFM and PH/C8/ZnO-C8/HFM was investigated using X-ray diffraction (XRD) thin film analysis. X-ray analysis revealed that the major phase of the sintered ball clay-based ceramic hollow fibre membrane is mullite along with minor constituent of cristabolite. The reduction in crystallinity of the mullite substrate, as shown in Fig. 8, indicates that ZnO particles were successfully deposited. The deposition of ZnO is further confirmed by the crystalline phase of ZnO having peaks arising at 2θ values of 32°, 35° and 37°, which were assigned to 100, 002 and 101, respectively [44].

3.3. Pore size and liquid entry pressure (LEP_w)

MIP analysis was performed to provide complete information about the membrane pore structure (pore size and total porosity) across the entire membrane, allowing the effect of coating layer deposition on the pore properties to be evaluated. The pore size distribution of the C8/HFM and PH/C8/ZnO-C8/HFM is shown in Fig. 9**(a)**. The results indicate that the pore size distributions of both samples are nearly identical, with only a slight reduction in pore size distribution area between 10 and 20 μm for PH/C8/ZnO-C8/HFM, which is most likely due to the addition of a coating layer. Both membranes have three peaks in the pore size distribution, which can be attributed to the sponge layer, micro-void, and lumen of the hollow fibre membrane. Sponge-like and micro-void structures were observed for both membranes at the ranges of 0.1–0.4 μm and 0.4–12 μm, respectively. The wetting resistance of both membranes was determined using the liquid entry pressure (LEP_w) technique. Because LEP_w exceedance is one of the most common causes of wetting, precise LEP_w estimation is required to avoid wetting in membrane distillation. Membrane properties such as water contact angle and maximum pore size can all have an impact on the LEP_w. As shown in Fig. 9**(b)**, an increase in LEP_w was observed from 0.37 ± 0.1 bar to 1.33 ± 0.4 bar, which could be attributed to some of the pores on the substrate surface being blocked after the surface coating with a PH/C8/ZnO layer.

3.4. Surface hydrophobicity

The wetting behaviours of all membranes were also investigated by measuring the contact angles of five different liquids with different surface energies. The contact angle value shown in Fig. 10 **(a-b)** was measured immediately after the liquid was dropped. All membranes are anti-wetting in both polar (water, water/ethanol, and ethylene glycol) and non-polar (palm oil and silicon oil) liquids. C8/HFM and PH/C8/ZnO-C8/HFM have super-hydrophobicity with contact angle of 151.7° and 154.4° respectively, but the latter has better contact angle hysteresis (CAH), implying that the PH/C8/ZnO-C8/HFM (CAH = 3.24°) surface is more slippery than the C8/HFM (CAH = 9.17°) surface **(See** Fig. 10**(c-f))** [45]. According to Eral et al. [46], hysteresis affects to the motion of the liquid which induce the slippery of the modified membrane. Interestingly, the C8/HFM effortlessly demonstrated superhydrophobic

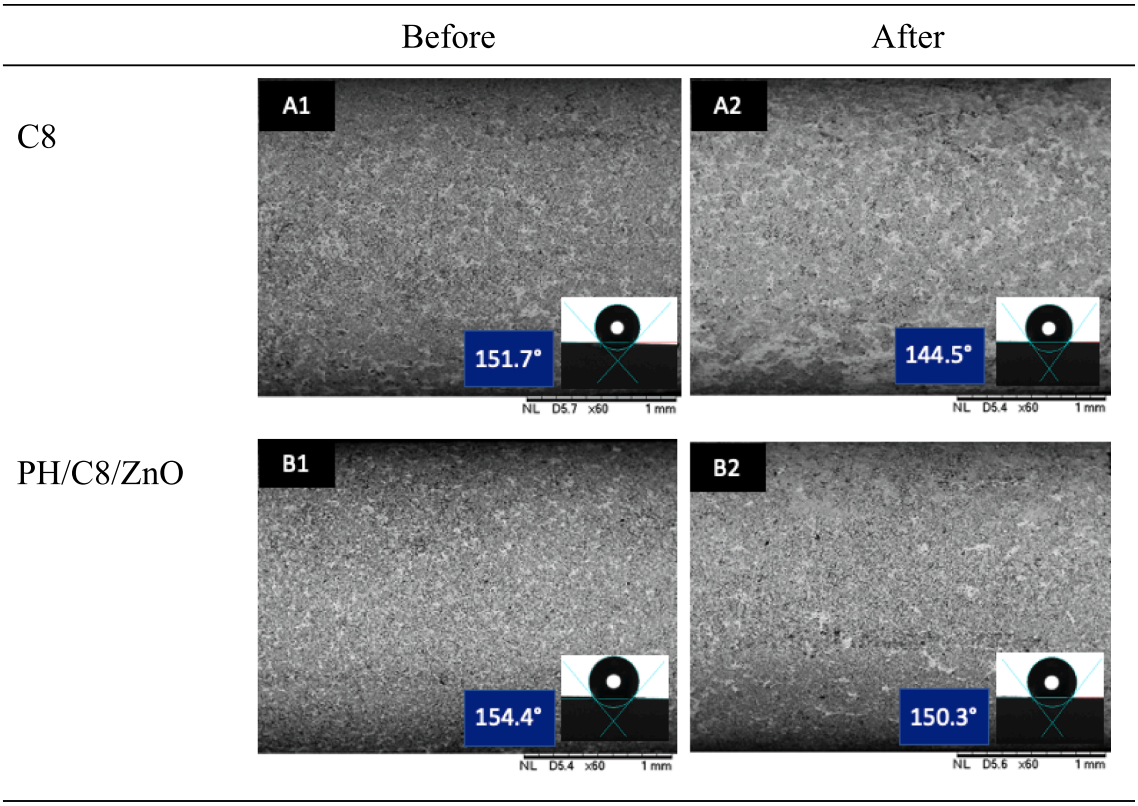

Fig. 12. SEM images and contact angle value for before and after MD test for C8 (**a1** and **a2**) and PH/C8/ZnO (**b1** and **b2**).

properties (>150°), and the contact angle result is better than that of most previously reported hydrophobic ceramic membranes without secondary structure on their surface (see Table 3). Meanwhile, when different liquids with different total surface energies were dropped on the membranes' surface, the PH/C8/ZnO-C8/HFM demonstrated better antiwetting properties for polar liquids (water and ethylene glycol), whereas the C8/HFM demonstrated better antiwetting properties for non-polar liquids (palm oil and silicon oil). It was hypothesized that the presence of non-polar polymeric material on the membrane surface from the adhesive PVDF-HFP has resulted in favourable interactions with non-polar liquids at the interface, resulting in a lower oil contact angle as compared to C8/HFM. Plus, with the addition of ZnO nanomaterial to the mixture also enhanced the anti-wetting properties of PH/C8/ZnO-C8/HFM due to interaction of ZnO and PVDF as also being reported from previous studies by Wang et al.[47] and Balta et al. [48]. Based on what has been reported from the studies, ZnO, a semiconductor material which also less toxic acts as anti-foulant, anti-corrosion and the material also easy to be embedded in the polymeric materials which induced the anti-wetting properties of the membrane. According to Figs. 9 and 10, the pore size and contact angle of the membrane before and after modification are not much different, but the LEPw of the modified membrane is significantly improved. It is postulated that the spray coated membrane's low hysteresis supports a metastable Cassie-Baxter surface, resulting in a "slippery" surface [49]. When water flows over such a surface, the flow resistance, which is determined by the contact surface and flow velocity at the membrane interface, can be significantly reduced, potentially improving the LEPw.

3.5. Membrane distillation

Surface coating frequently exhibits wetting resistance versus water vapour permeability trade-offs, as water vapour permeability typically decreases with increasing wetting resistance due to an external layer on the surface of a membrane [50]. In membrane distillation system, only vapour produced from the hot water (feed) was allowed to pass through the membrane's wall/surface to react with cold water (permeate), while NaCl was rejected or remained as retentate. The surface of the membrane must be equipped with hydrophobic to prevent water from feed to pass through the lumen side of the membrane. In order to assess the trade-off, the direct contact membrane distillation (DCMD) performance of C8/HFM and PH/C8/ZnO-C8/HFM was tested for 5 h using a NaCl aqueous solution (10 g/L) as a feed. A similar trade-off was observed in this study, where vapour permeability decreased with increasing wetting resistance (C8/HFM > PH/C8/ZnO-C8/HFM), as shown in Fig. 11. PH/C8/ZnO-C8/HFM has slightly lower fluxes than C8/HFM due to an additional layer of coating that may increase mass transfer resistance at the liquid–air-solid interface [22]. Though vapour permeability was slightly reduced for PH/C8/ZnO-C8/HFM, the rejection performance was better than C8/HFM because the coating layer may improve the hindrance of salt movement. Moreover, membrane wetting was never observed for both membranes throughout the duration of the MD operation. As depicted in Table 3, the C8/HFM and PH/C8/ZnO-C8/HFM demonstrated comparable vapour flux to ceramic hollow fibre membranes previously reported in the previous studies which average of 6.2 and 3.4 L/m^2.h for C8/HFM and PH/C8/ZnO-C8/HFM, respectively.

With the successful anchoring of a coating layer on ball clay based ceramic hollow fibre membrane with hierarchical structure via universal spray coating approach without compromising MD performance, this method appears to be a simpler to be applied for widespread application of superhydrophobic ceramic membrane in MD, as previous studies required process at elevated temperatures such as vapour-solid process [51], chemical bath deposition [23] and hydrothermal method [22]. Meanwhile, another simple method of fluorination via immersion method, most ceramic membranes do not appear to be capable of achieving superhydrophobicity, as summarised in Table 3. Thus, universal spray coating approach with a composite of PH/C8/ZnO proposed in this study can be a promising alternative.

In order to evaluate the properties of the membranes after MD test,

the membranes were subjected to SEM characterization to investigate any morphology changed and contact angle for hydrophobicity properties. As can be seen in Fig. 12 for before and after MD test, the C8/HFM (**a1** and **a2**) showed higher reduced of value of contact angle which the value reduced up to 7°. Compared to PH/C8/ZnO (**b1** and **b2**) the value of contact angle reduced only up to 4°. This output corresponds to previous study from Pauzan et al. [61] where from the study also depicted that the modification did not affect the performance of the membranes in MD especially the hydrophobicity of the membranes. In Fig. 12 also depicted that the morphology of the membranes did not affect much even after MD test which showed the capability of the membrane to be used in MD system.

4. Conclusions

This study reports the use of a universal spray coating method with a composite of PVDF-HFP, C8, and ZnO nanoparticles as a coating in the fabrication of a superhydrophobic ceramic hollow fibre membrane, in which ball clay was used as a low-cost ceramic material. Through this method, ball clay based ceramic hollow fibre membrane achieved superhydrophobicity: water contact angle and its hysteresis contact angle were measured to be 154.4 and 3.2°, respectively. Meanwhile, a higher hysteresis contact angle of 9.2° was observed for the C8/HFM. That is, PH/C8/ZnO-C8/HFM's surface is more slippery than that of C8/HFM. In terms of wetting resistance, the composite coating on the PH/C8/ZnO-C8/HFM significantly improved its LEP_w as compared to C8/HFM. However, a trade-off was observed, where vapour permeability decreased with increasing wetting resistance (C8/HFM > PH/C8/ZnO-C8/HFM). As compared to previously reported hydrophobic ceramic membranes in the body of literature, both membranes had comparable vapour flux and salt rejection with superhydrophobicity. When compared to other methods previously reported in the literature that require high temperature conditions [22,23,51], the alternative approach investigated in this study exhibits potential advantage to be a simpler method in achieving superhydrophobicity of ceramic membranes. In terms of directions for future research, further work could be carried out to verify the anti-wetting and anti-fouling properties of the membrane performances using feed liquids containing surfactants or oils as model foulants.

CRediT authorship contribution statement

Mohd Haiqal Abd Aziz: Writing – review & editing. **Mohammad Arif Budiman Pauzan:** Writing – review & editing. **Nur Aina Shazana Mohd Hisam:** Conceptualization, Methodology, Validation, Formal analysis, Investigation, Writing – review & editing. **Mohd Hafiz Dzarfan Othman:** Supervision, Writing – original draft, Conceptualization, Methodology, Investigation, Resources, Funding acquisition, Validation, Project administration, Writing – review & editing. **Mohd Ridhwan Adam:** Writing – review & editing, Methodology. **Yuji Iwamoto:** Writing – review & editing, Supervision. **Mohd Hafiz Puteh:** Writing – review & editing, Formal analysis, Supervision. **Mukhlis A Rahman:** Writing – review & editing, Supervision. **Juhana Jaafar:** Writing – review & editing, Supervision. **Ahmad Fauzi Ismail:** Writing – review & editing, Supervision. **Tonni Agustiono Kurniawan:** Writing – review & editing, Supervision, Formal analysis. **Suriani Abu Bakar:** Writing – review & editing, Supervision.

Declaration of Competing Interest

The authors declare that they have no known competing financial interests or personal relationships that could have appeared to influence the work reported in this paper.

Acknowledgement

The authors gratefully acknowledge the financial support from the Ministry of Science, Technology and Innovation (MOSTI) Malaysia through International Collaboration Fund (ICF) grant (Project Number: IF0120I1164 / R.J130000.4909.4S145), Ministry of Higher Education Malaysia under Higher Institution Centre of Excellence (HICoE) grant (Project Number: R.J090301.7809.4 J430) and Universiti Teknologi Malaysia under Matching Grant (Project Number: Q.J130000.3009.03 M15).

References

[1] C.B. Ong, L.Y. Ng, A.W. Mohammad, A review of ZnO nanoparticles as solar photocatalysts: synthesis, mechanisms and applications, Renew. Sustain. Energy Rev. 81 (2018) 536–551, https://doi.org/10.1016/j.rser.2017.08.020.
[2] M. Shadi, S. Abujazar, S. Fatihah, A.R. Rakmi, M.Z. Shahrom, The effects of design parameters on productivity performance of a solar still for seawater desalination : a review, Desalination 385 (2016) 178–193, https://doi.org/10.1016/j.desal.2016.02.025.
[3] N. Izzah, H.A. Aziz, M.M. Hana, Application of life cycle assessment for desalination : progress, challenges and future directions *, Environ. Pollut. 268 (2021), 115948, https://doi.org/10.1016/j.envpol.2020.115948.
[4] Y. Chen, K. Jia, T. Chung, An omniphobic slippery membrane with simultaneous anti-wetting and anti-scaling properties for robust membrane distillation, J. Memb. Sci. 595 (2020), 117572, https://doi.org/10.1016/j.memsci.2019.117572.
[5] D. Hou, C. Ding, K. Li, D. Lin, D. Wang, J. Wang, A novel dual-layer composite membrane with underwater-superoleophobic / hydrophobic asymmetric wettability for robust oil-fouling resistance in membrane distillation desalination, Desalination 428 (2018) 240–249, https://doi.org/10.1016/j.desal.2017.11.039.
[6] A. Deshmukh, et al., Membrane distillation at the water-energy nexus: limits, opportunities, and challenges, Energy Environ. Sci. 11 (5) (2018) 1177–1196, https://doi.org/10.1039/C8EE00291F.
[7] O. Gupta, S. Roy, S. Mitra, Enhanced membrane distillation of organic solvents from their aqueous mixtures using a carbon nanotube immobilized membrane, J. Memb. Sci. 568 (2018) 134–140, https://doi.org/10.1016/j.memsci.2018.10.002.
[8] M. Rezaei, D.M. Warsinger, M.C. Duke, T. Matsuura, W.M. Samhaber, Wetting phenomena in membrane distillation: mechanisms, reversal, and prevention, Water Res. 139 (2018) 329–352, https://doi.org/10.1016/j.watres.2018.03.058.
[9] Y. Zen, S. Velioglu, L. Han, B. Dannie, L. Gopalakrishnan, J. Wei, Effect of surfactant hydrophobicity and charge type on membrane distillation performance, J. Memb. Sci. 587 (2019), 117168, https://doi.org/10.1016/j.memsci.2019.117168.
[10] X. Li, H. Shan, M. Cao, B. Li, Facile fabrication of omniphobic PVDF composite membrane via a waterborne coating for anti-wetting and anti-fouling membrane distillation, J. Membr. Sci. 589 (2019), https://doi.org/10.1016/j.memsci.2019.117262.
[11] L. Chen, Z. Guo, W. Liu, Outmatching superhydrophobicity: bio-inspired re-entrant curvature for mighty superamphiphobicity in air, J. Mater. Chem. A 5 (28) (2017) 14480–14507, https://doi.org/10.1039/C7TA03248J.
[12] N. Dizge, E. Shaulsky, V. Karanikola, Electrospun cellulose nanofibers for superhydrophobic and oleophobic membranes, J. Memb. Sci. 590 (2019), 117271, https://doi.org/10.1016/j.memsci.2019.117271.
[13] X. Gou, Z. Guo, Surface topographies of biomimetic superamphiphobic materials : design criteria, fabrication and performance, Adv. Colloid Interface Sci. 269 (2019) 87–121, https://doi.org/10.1016/j.cis.2019.04.007.
[14] Y.L.E. Fung, H. Wang, Nickel aluminate spinel reinforced ceramic hollow fibre membrane, J. Memb. Sci. 450 (2014) 418–424, https://doi.org/10.1016/j.memsci.2013.09.036.
[15] J.-W. Zhang, H. Fang, J.-W. Wang, L.-Y. Hao, X. Xu, C.-S. Chen, Preparation and characterization of silicon nitride hollow fiber membranes for seawater desalination, J. Memb. Sci. 450 (2014) 197–206, https://doi.org/10.1016/j.memsci.2013.08.042.
[16] S. Salwa, M. Rao, K. Shyuan, Perovskite-based proton conducting membranes for hydrogen separation : a review, Int. J. Hydrogen Energy 3 (43) (2018), https://doi.org/10.1016/j.ijhydene.2018.06.045, 15281e15305.
[17] M.F.H. Me, M.H.A. Bakar, Tubular ceramic performance as separator for microbial fuel cell : a review, Int. J. Hydrogen Energy 5 (45) (2019), https://doi.org/10.1016/j.ijhydene.2019.08.115, 22340e22348.
[18] S.K. Hubadillah, Z.S. Tai, M.H.D. Othman, Z. Harun, M.R. Jamalludin, M. A. Rahman, J. Jaafar, A.F. Ismail, Hydrophobic ceramic membrane for membrane distillation: a mini review on preparation, characterization, and applications, Sep. Purif. Technol. 217 (2019) 71–84, https://doi.org/10.1016/j.seppur.2019.02.014.
[19] N.A. Ahmad, C.P. Leo, A.L. Ahmad, Superhydrophobic alumina membrane by steam impingement: minimum resistance in microfiltration, Sep. Purif. Technol. 107 (2013) 187–194, https://doi.org/10.1016/j.seppur.2013.01.011.
[20] L. Li, J.-W. Wang, H. Zhong, L.-Y. Hao, H. Abadikhah, X. Xu, C.-S. Chen, S. Agathopoulus, Novel α -Si3N4 planar nanowire superhydrophobic membrane prepared through in-situ nitridation of silicon for membrane distillation, J. Memb. Sci. 543 (April) (2017) 98–105, https://doi.org/10.1016/j.memsci.2017.08.049.

[21] T. Wang, Y. Yun, M. Wang, C. Li, Superhydrophobic ceramic hollow fiber membrane planted by ZnO nanorod-array for high-salinity water desalination, J. Taiwan Inst. Chem. Eng. 105 (2019) 17–27, https://doi.org/10.1016/j.jtice.2019.10.009.
[22] M.H. Abd Aziz, M.H.D. Othman, N.H. Alias, T. Nakayama, Y. Shingaya, N. A. Hashim, T.A. Kurniawan, T. Matsuura, M. A. Rahman, J. Jaafar, Enhanced omniphobicity of mullite hollow fiber membrane with organosilane-functionalized TiO2 micro-flowers and nanorods layer deposition for desalination using direct contact membrane distillation, J. Memb. Sci. 607 (April) (2020), 118137, https://doi.org/10.1016/j.memsci.2020.118137.
[23] L.H. Chen, Y.R. Chen, A. Huang, C.H. Chen, D.-Y. Su, C.-C. Hsu, F.-Y. Tsai, K.-L. Tung, Nanostructure depositions on alumina hollow fiber membranes for enhanced wetting resistance during membrane distillation, J. Memb. Sci. 564 (July) (2018) 227–236, https://doi.org/10.1016/j.memsci.2018.07.011.
[24] Y. Liao, G. Zheng, J. Jeanne, M. Tian, R. Wang, Development of robust and superhydrophobic membranes to mitigate membrane scaling and fouling in membrane distillation, J. Memb. Sci. 601 (2020), 117962, https://doi.org/10.1016/j.memsci.2020.117962.
[25] X. Li, X. Yu, C. Cheng, L. Deng, M. Wang, X. Wang, Electrospun Superhydrophobic Organic / Inorganic Composite Nanofibrous Membranes for Membrane Distillation, ACS Appl. Mater. Interfaces 7 (39) (2015) 21919–21930, https://doi.org/10.1021/acsami.5b06509.
[26] B.J. Deka, J. Guo, N.K. Khanzada, A.K. An, Omniphobic re-entrant PVDF membrane with ZnO nanoparticles composite for desalination of low surface tension oily seawater, Water Research 165 (2019) 1–12, https://doi.org/10.1016/j.watres.2019.114982.
[27] M. Wen, et al., Superhydrophobic composite graphene oxide membrane coated with fluorinated silica nanoparticles for hydrogen isotopic water separation in membrane distillation, J. Memb. Sci. 626 (November) (2020) 2021, https://doi.org/10.1016/j.memsci.2021.119136.
[28] Z. Liu, Q. Pan, C. Xiao, Preparation and vacuum membrane distillation performance of a silane coupling agent-modified polypropylene hollow fiber membrane, Desalination 468 (2019), https://doi.org/10.1016/j.desal.2019.06.026.
[29] C. Li, W. Sun, Z. Lu, X. Ao, S. Li, Ceramic nanocomposite membranes and membrane fouling: a review, Water Res. 175 (2020), 115674, https://doi.org/10.1016/j.watres.2020.115674.
[30] D. Das, S. Baitalik, B. Haldar, R. Saha, N. Kayal, Preparation and characterization of macroporous SiC ceramic membrane for treatment of waste water, J. Porous Mater. 25 (4) (2018) 1183–1193, https://doi.org/10.1007/s10934-017-0528-5.
[31] M.H. Abd Aziz, M.H.D. Othman, N.A. Hashim, M.R. Adam, A. Mustafa, Fabrication and characterization of mullite ceramic hollow fiber membrane from natural occurring ball clay, Appl. Clay Sci. 177 (May) (2019) 51–62, https://doi.org/10.1016/j.clay.2019.05.003.
[32] R. Ali, K. Rao, M. Kashifuddin, Adsorption studies of Cd (II) on ball clay : Comparison with other natural clays, Arab. J. Chem. 9 (2016) 1233–1241, https://doi.org/10.1016/j.arabjc.2012.01.010.
[33] S.K. Hubadillah, et al., Removal of As(iii) and As(v) from water using green, silica-based ceramic hollow fibre membranes: via direct contact membrane distillation, RSC Adv. 9 (6) (2019) 3367–3376, https://doi.org/10.1039/C8RA08143C.
[34] A. El-gendi, F.A. Samhan, N. Ismail, L.A.N. El-dein, Synergistic role of Ag nanoparticles and Cu nanorods dispersed on graphene on membrane desalination and biofouling, J. Ind. Eng. Chem. 65 (2018) 127–136, https://doi.org/10.1016/j.jiec.2018.04.021.
[35] D. Hou, G. Dai, J. Wang, H. Fan, Z. Luan, C. Fu, Boron removal and desalination from seawater by PVDF flat-sheet membrane through direct contact membrane distillation, Desalination 326 (2013) 115–124, https://doi.org/10.1016/j.desal.2013.07.023.
[36] K. Karpagavel, K. Sundaramahalingam, A.M.D. Vanitha, A.M.E.R. Nagarajan, Electrical Properties of Lithium - Ion Conducting Poly (Vinylidene Fluoride - Co - Hexafluoropropylene) (PVDF - HFP)/ Polyvinylpyrrolidone (PVP) Solid Polymer Electrolyte, J. Electron. Mater. (2021), https://doi.org/10.1007/s11664-021-08967-9.
[37] S. Badatya, A. Kumar, C. Sharma, A. Kumar, Transparent flexible graphene quantum dot- (PVDF-HFP) piezoelectric nanogenerator, Mater. Lett. 290 (2021), 129493, https://doi.org/10.1016/j.matlet.2021.129493.
[38] M. Lin, P. See, Formation of PVDF-g-HEMA/BaTiO3 nanocomposites via in situ nanoparticle synthesis for high performance capacitor applications, J. Mater. Chem. A 1 (2013) 14455–14459, https://doi.org/10.1039/C3TA13190D.
[39] L. Yesappa, et al., Optical properties and ionic conductivity studies of an 8 MeV electron beam irradiated poly(vinylidene fluoride-co-hexafluoropropylene)/LiClO4 electrolyte film for opto-electronic applications, RSC Adv. 8 (2004) (2018) 15297–15309, https://doi.org/10.1039/C8RA00970H.
[40] S. Radhika, J. Thomas, Solar light driven photocatalytic degradation of organic pollutants using ZnO nanorods coupled with photosensitive molecules, J. Environ. Chem. Eng. 5 (May) (2017) 4239–4250, https://doi.org/10.1016/j.jece.2017.08.013.
[41] M. Stan, A. Popa, D. Toloman, T.D. Silipas, D.C. Vodnar, Antibacterial and antioxidant activities of ZnO nanoparticles synthesized using extracts of Allium sativum, Rosmarinus officinalis and Ocimum basilicum, Acta Metall. Sin. (English Lett. 29 (3) (2016) 228–236, https://doi.org/10.1007/s40195-016-0380-7.
[42] X. Wu, X. Wu, T. Wang, L. Zhao, Y. Bach, Omniphobic surface modification of electrospun nanofiber membrane via vapor deposition for enhanced anti-wetting property in membrane distillation, J. Memb. Sci. 606 (January) (2020), 118075, https://doi.org/10.1016/j.memsci.2020.118075.
[43] H. Fu, X. Ding, C. Ren, W. Li, H. Yang, Preparation of magnetic porous NiFe2O4/SiO2 composite xerogels for potential application in adsorption of Ce(IV) ions from aqueous solution, RSC Adv. 7 (3) (2017) 16513–16523, https://doi.org/10.1039/C6RA27219C.
[44] A.K. Zak, R. Razali, Synthesis and characterization of a narrow size distribution of zinc oxide nanoparticles, Int. J. Nanomedicine 6 (2011) 1399–1403, https://doi.org/10.2147/IJN.S19693.
[45] L. Gao, T.J. McCarthy, Contact Angle Hysteresis Explained, Langmuir 22 (14) (Jul 2006) 6234–6237, https://doi.org/10.1021/la060254j.
[46] H.B. Eral, D.J.C.M. 't, Mannetje, J.M. Oh, Contact angle hysteresis: a review of fundamentals and applications, Colloid Polym. Sci., Feb. 291 (2) (2013) 247–260, https://doi.org/10.1007/s00396-012-2796-6.
[47] M. Wang, et al., ZnO Nanorod Array Modified PVDF Membrane with Superhydrophobic Surface for Vacuum Membrane Distillation Application, ACS Appl. Mater. Interfaces 10 (16) (Apr 2018) 13452–13461, https://doi.org/10.1021/acsami.8b00271.
[48] S. Balta, A. Sotto, P. Luis, L. Benea, B. Van Der Bruggen, J. Kim, A new outlook on membrane enhancement with nanoparticles : the alternative of ZnO, J. Memb. Sci. 389 (2012) 155–161, https://doi.org/10.1016/j.memsci.2011.10.025.
[49] A. Giacomello, M. Chinappi, S. Meloni, C.M. Casciola, Metastable Wetting on Superhydrophobic Surfaces: continuum and Atomistic Views of the Cassie-Baxter–Wenzel Transition, Phys. Rev. Lett. 109 (22) (Nov. 2012), 226102, https://doi.org/10.1103/PhysRevLett.109.226102.
[50] W. Wang, et al., Trade-off in membrane distillation with monolithic omniphobic membranes, Nat. Commun. 10 (1) (2019) 1–9, https://doi.org/10.1038/s41467-019-11209-6.
[51] L. Li, H. Abadikhah, J.W. Wang, X. Xu, S. Agathopoulos, One-step synthesis of flower-like Si2N2O nanowires on the surface of porous SiO2 ceramic membranes for membrane distillation, Mater. Lett. 232 (2018) 74–77, https://doi.org/10.1016/j.matlet.2018.08.043.
[52] R. Das, K. Sondhi, S. Majumdar, S. Sarkar, Development of hydrophobic clay–alumina based capillary membrane for desalination of brine by membrane distillation, J. Asian Ceram. Soc. 4 (3) (Sep. 2016) 243–251, https://doi.org/10.1016/j.jascer.2016.04.004.
[53] J.W. Wang, et al., Porous B-Sialon planar membrane with a robust polymer-derived hydrophobic ceramic surface, J. Memb. Sci. 535 (2017) 63–69, https://doi.org/10.1016/j.memsci.2017.04.028.
[54] Y.X. Huang, Z. Wang, D. Hou, S. Lin, Coaxially electrospun super-amphiphobic silica-based membrane for anti-surfactant-wetting membrane distillation, J. Membr. Sci. 531 (2017) 122–128, https://doi.org/10.1016/j.memsci.2017.02.044.
[55] S.K. Hubadillah, M.H.D. Othman, Z. Harun, A.F. Ismail, M.A. Rahman, J. Jaafar, A novel green ceramic hollow fiber membrane (CHFM) derived from rice husk ash as combined adsorbent-separator for efficient heavy metals removal, Ceram. Int. 43 (5) (Apr. 2017) 4716–4720, https://doi.org/10.1016/j.ceramint.2016.12.122.
[56] S. Cong, X. Liu, F. Guo, Membrane distillation using surface modified multi-layer porous ceramics, Int. J. Heat Mass Transf. 129 (2019) 764–772, https://doi.org/10.1016/j.ijheatmasstransfer.2018.10.011.
[57] M. Yang, J. Wang, L. Li, B. Dong, X. Xu, S. Agathopoulos, Fabrication of low thermal conductivity yttrium silicate ceramic flat membrane for membrane distillation, J. Eur. Ceram. Soc. 39 (2019) 442–448, https://doi.org/10.1016/j.jeurceramsoc.2018.09.028.
[58] B. Dong, et al., Polymer-derived porous SiOC ceramic membranes for e ffi cient oil-water separation and membrane distillation, J. Memb. Sci. 579 (2019) 111–119, https://doi.org/10.1016/j.memsci.2019.02.066.
[59] M. Pagliero, A. Bottino, A. Comite, C. Costa, Silanization of tubular ceramic membranes for application in membrane distillation, J. Memb. Sci. 601 (2020) 1–10, https://doi.org/10.1016/j.memsci.2020.117911.
[60] H. Aloulou, W. Aloulou, M.O. Daramola, R. Ben Amar, Silane-grafted sand membrane for the treatment of oily wastewater via air gap membrane distillation: study of the efficiency in comparison with microfiltration and ultrafiltration ceramic membranes, Mater. Chem. Phys. vol. 261, no. January (2021), 124186, https://doi.org/10.1016/j.matchemphys.2020.124186.
[61] M.A.B. Pauzan, S.K. Hubadillah, S.N.E.A.M. Kamal, M.H.D. Othman, M.H. Puteh T. A. Kurniawan, S.A. Bakar, H. Abdullah, M.R. Jamalludin, R. Naim, S.H.S.A. Kadir, Novel ceramic hollow fibre membranes contactor derived from kaolin and zirconia for ammonia removal and recovery from synthetic ammonia, J. Membr. Sci. 638 (2021), https://doi.org/10.1016/j.memsci.2021.119707.